Super-Exchange Charge Transfer in One-Photon and Two-Photon Absorption of Multibranched Compounds

Xinyue Wang, Di Wang, Jia Li, Meixia Zhang, Dawei Kang,* and Peng Song*

ACCESS | Metrics & More | Article Recommendations

ABSTRACT: In this work, density functional theory is used to study organic molecules in a donor−acceptor (D−A) system centered on phenothiazine with strip and trigonal structures. The transition modes of the one-photon absorption (OPA) and two-photon absorption (TPA) processes of the two molecules are studied. The calculations show that the molar absorption coefficient of OPA for trigonal molecule TPPO and the cross section of TPA are both larger than those for strip molecule M1 due to the increase in the number of branches of the system. A special local excitation-enhanced charge-transfer excitation appears in strip-type molecule M1. In the charge-transfer process of trigonal D−A structure molecule TPPO, there are not only local excitation-enhanced charge-transfer excitation but also super-exchange charge transfer between the three branches that occurs due to the increase in the planarity of the system.
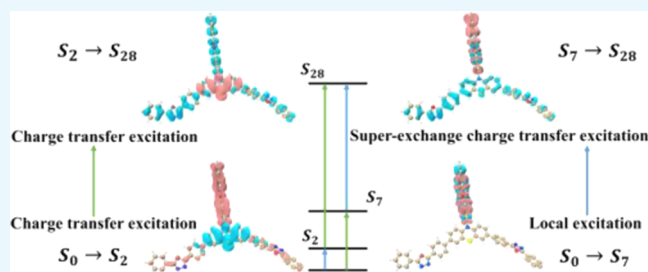
1. INTRODUCTION

Two-photon absorption (TPA) induces the transformation of molecules into excited electronic states by simultaneously absorbing and combining two low-energy photons (the energies of the two photons can be the same or different), which is a third-order nonlinear process.[1] However, under a high-power beam, using a light source approaching twice the linear absorption wavelength of the molecule to excite the molecule can also excite the same transition. Göppert−Mayer[2] first proposed the TPA theory in 1931. Kaiser and Garret[3] first verified the existence of TPA from a two-photon excitation experiment in 1962. TPA is characterized by its absorption intensity, which is proportional to the square of the incident light intensity. The long-wavelength absorption and short-wave-length emission of two-photon absorption allow the high penetration rate of light waves, which greatly reduces the dissipation and destruction of excitation light by the medium. The excellent optical properties of these organic nonlinear optical materials in the TPA process make them promising for applications, including dye-sensitized solar cells,[4−7] two-photon fluorescence microscopes,[8−12] optical data storage,[13−15] and photodynamic therapy.[12,16−20]

Many researchers have proposed methods of constructing TPA molecules in terms of molecular configuration and TPA characteristics to enhance the charge transfer within the molecule. It is common to construct a donor−acceptor (D−A) structure and increase the push−pull electron strength between substituents,[1,21−23] connect the two through conjugated linkers,[24−27] and construct molecules of different chiralities[28] and organic multibranched two-photon absorbing molecules with cores and branches.[29] Qiao, Mu, and co-workers reported that the triangular axial type of 1,3,5-triazine derivatives has a larger 2PA cross section compared to the striped and V-type.[30] In recent years, due to its nonplanar "butterfly" structure, phenothiazine can effectively inhibit the self-stacking of dye molecules to obtain higher photovoltage. Therefore, it is often used to design and synthesize various dye photosensitizers,[31,32] solar cells,[33,34] fluorescent probes,[35,36] and stimulus-responsive materials.[37] Meanwhile, the presence of nitrogen and sulfur heteroatoms in the molecule makes it more electron-donating, and multibranched molecules containing heteroatoms have larger π-domains and more pronounced multipolar features. Therefore, in this work, the TPA properties of strip and trigonal structures were studied with phenothiazine as an electron donor, and the effect of increasing the number of branches on the TPA properties was investigated.

In this work, we theoretically studied the TPA process of two phenothiazine derivatives with phenothiazine as a donor and oxadiazole end groups as an acceptor. With the central donor of phenothiazine, the oxadiazole end group is branched to form D−A strip structure molecule 1 and trigonal structure molecule 2, following the previous work of Wu et al.[38] The first molecule is
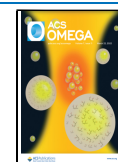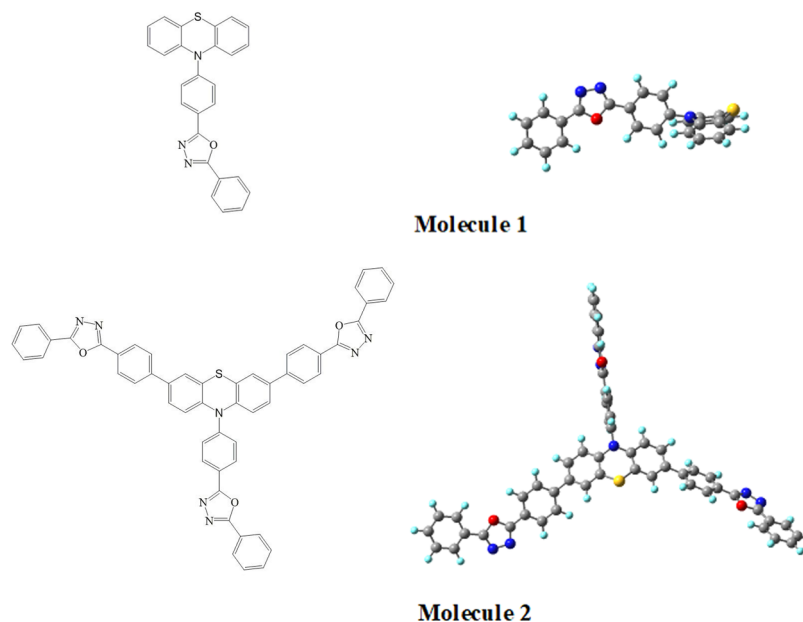
Figure 1. Two-dimensional structure diagrams (left) and the optimized geometric configuration diagrams (right) of molecules 1 and 2.

2-(4-(10-phenothiazinyl)benzene)-5-phenyl-1,3,4-oxadiazole (M1), and its branch is connected to the bond at position 10 of phenothiazine. The second molecule is 3,7,10-triplet(4-(2-phenyl-1,3,4-oxadiazole phenyl)) (TPPO), and its branches are connected to positions 3, 7, and 10 of phenothiazine, forming a trigonal structure. The optimized geometric configurations of M1 and TPPO are shown in Figure 1. First, by simulating the UV−vis and TPA spectra of one-photon absorption (OPA), the influence on the increase in the number of branches on the one-photon and TPA characteristics are analyzed. The TPA spectrum and the search for the intermediate state were achieved using the program developed by Mu and Sun based on the sum-of-states (SOS) model.[39] In this process, the influence of the increase in the number of branches on the one-photon and TPA characteristics are discussed for the emergence of super-exchange charge transfer different from the conventional ones, and the relationship between the structure and properties of charge transfer is understood in theory. Our study provides a theoretical basis for the design and synthesis of TPA materials and has good application prospects.

2. METHOD

2.1. Calculation Details. All quantum chemistry calculations were performed with the Gaussian 09 D.01 software package.[40] Using the B3LYP functional and the 6-31G(d) basis sets, with the density functional theory (DFT) method,[41−43] the molecular geometry of the ground state was optimized. The time-dependent DFT (TD-DFT)/B3LYP method is poor in the charge-transfer (CT) excitation calculation. Therefore, to calculate the electronic transitions of the two molecules, TD-DFT was used, on the theoretical level of CAM-B3LYP/TZVP.[44−46] According to the TPA spectrum and absorption cross section obtained by the program developed by Mu and Sun,[39] the two-dimensional (2D) charge-transfer matrix (CTM) and transition-density matrix (TDM) and three-dimensional (3D) charge-density difference (CDD) of each excited state and each path are obtained through the Multiwfn 3.7 program.[47] The 3D isosurface of the CDD map drawn using VMD software[48] can intuitively display the direction of charge transfer.

2.2. Two-Photon Absorption. Microscopically, the ratio of the molecular transition probability per unit time to the square of the photon flux is the cross section of the TPA to measure the size of the TPA. Based on the sum-of-states (SOS) model, TPA involves two absorption processes; the first process is to induce the molecule to transform into an excited state, and then to transition to a higher excited state. So, in the two-photon transition process, there will be different paths to the final state, and the absorption probability (δ_{tp}) is calculated by the sum-of-states (SOS) model that is the sum of the processes through all intermediate states.[49−51]

$$\delta_{tp} = 8 \sum_{\substack{j\neq g \\ j\neq f}} \frac{|\langle f|u|j\rangle|^2 |\langle j|u|g\rangle|^2}{(w_j - w_f/2)^2 + \Gamma_f^2}(1 + 2\cos^2\theta_j)$$
$$+ 8\frac{|\Delta u_{fg}|^2 |\langle f|u|g\rangle|^2}{(w_f/2)^2 + \Gamma_f^2}(1 + 2\cos^2\phi) \quad (1)$$

where g is the ground state, j is the intermediate state, f is the final state, $|g\rangle$, $|j\rangle$, and $|f\rangle$ are the wave functions of the three states, and w is the energy; the transition dipole moments of the two processes are expressed as $\langle f|u|j\rangle$ and $\langle j|u|g\rangle$, respectively. Here, $\langle g|u|g\rangle$ and $\langle f|u|f\rangle$ are the permanent dipole moments of the g and f states, respectively, and Δu_{fg} is the difference between the two. θ_j is the angle between $\langle j|u|g\rangle$ and $\langle f|u|j\rangle$, ϕ is the angle between Δu_{fg} and $\langle f|u|g\rangle$, and Γ_f is the TPA spectral line width. The first term of the formula is called the "three-state" term, and the second term is called the "two-state" term, which, respectively, represent the contribution of two-step transition and one-step transition to the absorption probability.

The cross section measuring the size of TPA[52,53] is

$$\sigma_{tp} = \frac{4\pi^2 a_0^5 \alpha}{15 c_0} \frac{w^2 g(w)}{\Gamma_f} \delta_{tp} \quad (2)$$

where w is the energy of the incident light, a_0 is the Bohr radius, α is the fine structure constant, c_0 is the speed of light, and $g(w)$ is the contour of the spectral line.
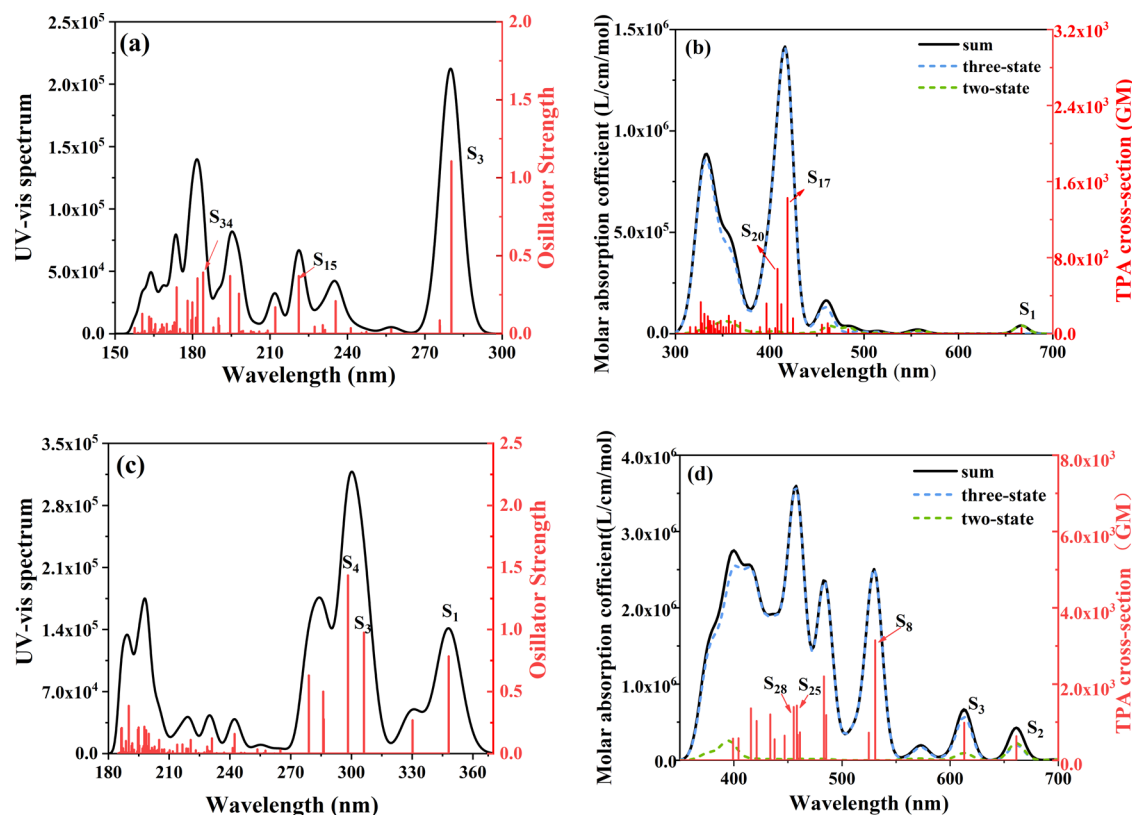
Figure 2. OPA UV−vis and TPA spectrum of M1 (a, b) and TPPO (c, d). The black, blue, and green lines in (c, d) represent the sum, "three-state", and "two-state" terms, respectively.

2.3. Transition-Density Matrix, Charge-Transfer Matrix, and Charge-Density Difference. The TDM can be used to calculate the transition density to analyze the coherence of atoms in the molecule to determine the excitation mode.

In real space, under a specific set of basis functions, the TDM can be constructed as[39]

$$T(r; r') = \sum_\mu \sum_\nu P_{\mu\nu}^{\text{tran}} \chi_\mu(r) \chi_\mu(r') \tag{3}$$

Assuming that the system only has u and v, the charge-transfer process is expressed as the transition of i (unoccupied orbital) $\rightarrow$ j (occupied orbital) using these two basis functions, and the TDM at this time

$$p_{uv}^{\text{tran}} = \begin{bmatrix} C_{vi}C_{\mu i} & C_{vi}C_{vj} \\ C_{\mu i}C_{\mu j} & C_{vi}C_{ui} \end{bmatrix} \tag{4}$$

If the absolute value of the diagonal element is large, the same basis function makes a large contribution to holes and electrons. In other words, holes and electrons have a significant overlap in this basis function, so the excitation is local excitation. If the off-diagonal elements are relatively large, it means that basis functions are strongly coupled during this process, which means that charge-transfer excitation has occurred.

The CTM is an effective 2D tool. The number of electrons transferred from R to S is calculated using the IFCT method.[46]

$$Q_{R,S} = \Theta_{R,\text{hole}}\Theta_{S,\text{ele}} \tag{5}$$

where $\Theta_{R,\text{hole}}$ is the amount of R occupied by the excited electrons, $\Theta_{S,\text{ele}}$ is the amount occupied by S where the election is going, and the product of the two is defined as the number of

electrons transferred from R to S. The more holes R occupies and the more electrons S occupies, the more electrons are transferred from R to S. The diagonal element of the CTM is in the form of "the number of electrons transferred by the fragment to itself," and each nondiagonal element strictly shows the amount of electron transfer between atoms.

Because the TPA process will experience different intermediate states, the CDD can intuitively show where the electrons have gone and how much has been transferred, so this is a good way to observe the charge-transfer process in 3D space. First, a density matrix of excited states is generated as follows[39]

$$P^{\text{excited}} = P^{\text{ground}} + \sum_{i \rightarrow j} (w_i^j)^2 (P^j - P^i)$$
$$+ \sum_{i \leftarrow j} (w_i^j)^2 (P^j - P^i) \tag{6}$$

Among them, P^{ground} and P^{excited} are the density matrices of the wave functions of the unexcited state and the excited state, respectively, and P^i and P^j are the density matrices contributed by i and j, respectively. Then, the density matrix is diagonalized to generate a natural orbital, and finally, the CDD is obtained by difference.

3. RESULTS AND DISCUSSION

3.1. Absorption Spectrum of OPA and TPA. The OPA UV−vis and TPA spectra for molecules 1 and 2 are shown in Figure 2a−d. Figure 2a,c shows the OPA spectra of M1 and TPPO, respectively. The left axis of the one-photon absorption spectrum represents the molar absorption intensity of the OPA process, and the right axis represents the oscillator intensity. As shown in Figure 2a, the OPA (UV−vis) spectrum of M1 consists
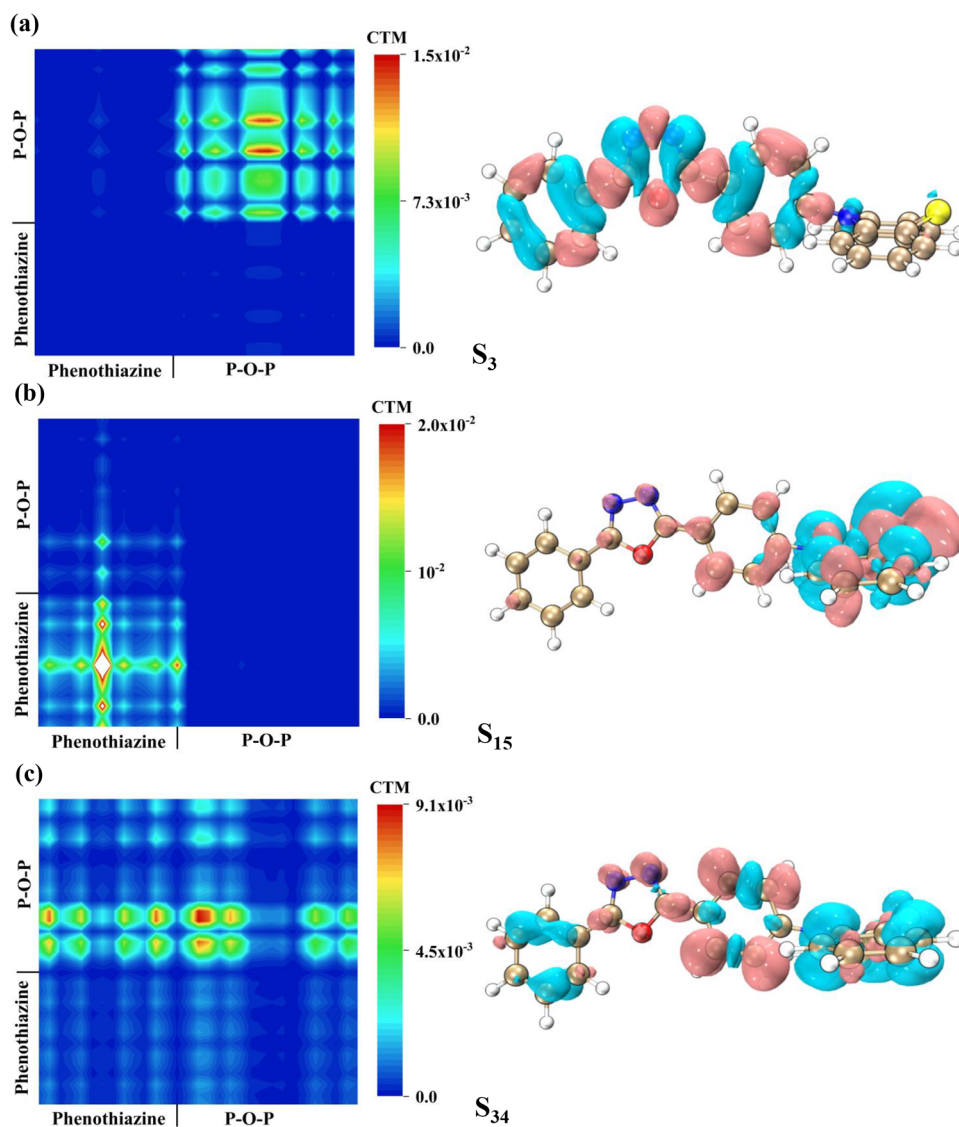
Figure 3. CTM and CDD for the S_3 (a), S_{15} (b), and S_{34} (c) excited states of M1; in CDD, pink represents electrons and blue represents holes.

of the strongest absorption peak, and many weak absorption peaks in the lower wavelength range, with its strongest absorption peak contributed by the S_3 excited state. In contrast, TPPO has two other weak absorption peaks in the 315−370 nm range, consisting of S_1 and S_2, and its strongest absorption peak is mainly contributed by S_3 and S_4 together. Comparing the UV−vis spectrum of the two molecules, it can be seen that the absorption wavelength to the third excited state of M1 is 280.07 nm and the wavelength of TPPO is 305.91 nm. Therefore, it can be concluded that an increase in the number of branches leads to a red shift of the spectrum of the molecule. It can be seen that the molar absorption coefficient of TPPO is larger than that of M1, that is, as the number of branches increases, the absorption intensity of the molecule increases. For the excited state with intermediate energy, the OPA characteristic is not obvious but it may undergo the second process of TPA, be induced to a higher excited state, and finally undergo the TPA transition process.

Figure 2b,d shows the TPA spectrum of the two molecules obtained using the three-state model. The left axis represents the absorption intensity (molar absorption coefficient) of the TPA process and the right axis represents the absorption cross section (the sum of the first and second terms in eq 1). The complete

TPA process is represented by a black solid line. The blue dotted line represents the "three-state" term, which is divided into two steps: the ground-state molecule transitions to the excited state by absorbing photons and then is induced to the final state, which can be expressed as $S_g \rightarrow S_j \rightarrow S_f$. The green dotted line represents the "two-state" term, which is a one-step transition without an intermediate state: a direct transition to the final state, which can be expressed as $S_g \rightarrow S_f$. According to the TPA spectra of the two molecules, the first term accounts for the main part. As shown in Figure 2b,d, the TPA spectrum of M1 is mainly composed of main peaks and side peaks, and its strongest absorption peak is mainly contributed by S_{20} and S_{17}. However, the TPA spectrum of TPPO is much more complicated than that of M1, and the TPA cross-sectional value of TPPO at 530 nm is 3149 GM, while that of M1 at 418 nm is 1427 GM. This shows that the planarity of the multibranched molecule may enhance the TPA cross-sectional values. It can be seen that the TPA spectrum of TPPO is the same as OPA and that the TPA peak has a significant red shift.

3.2. One-Photon Absorption. The increase in the number of branches of the two molecules centered on phenothiazine caused significant changes in the spectra of OPA and TPA. To
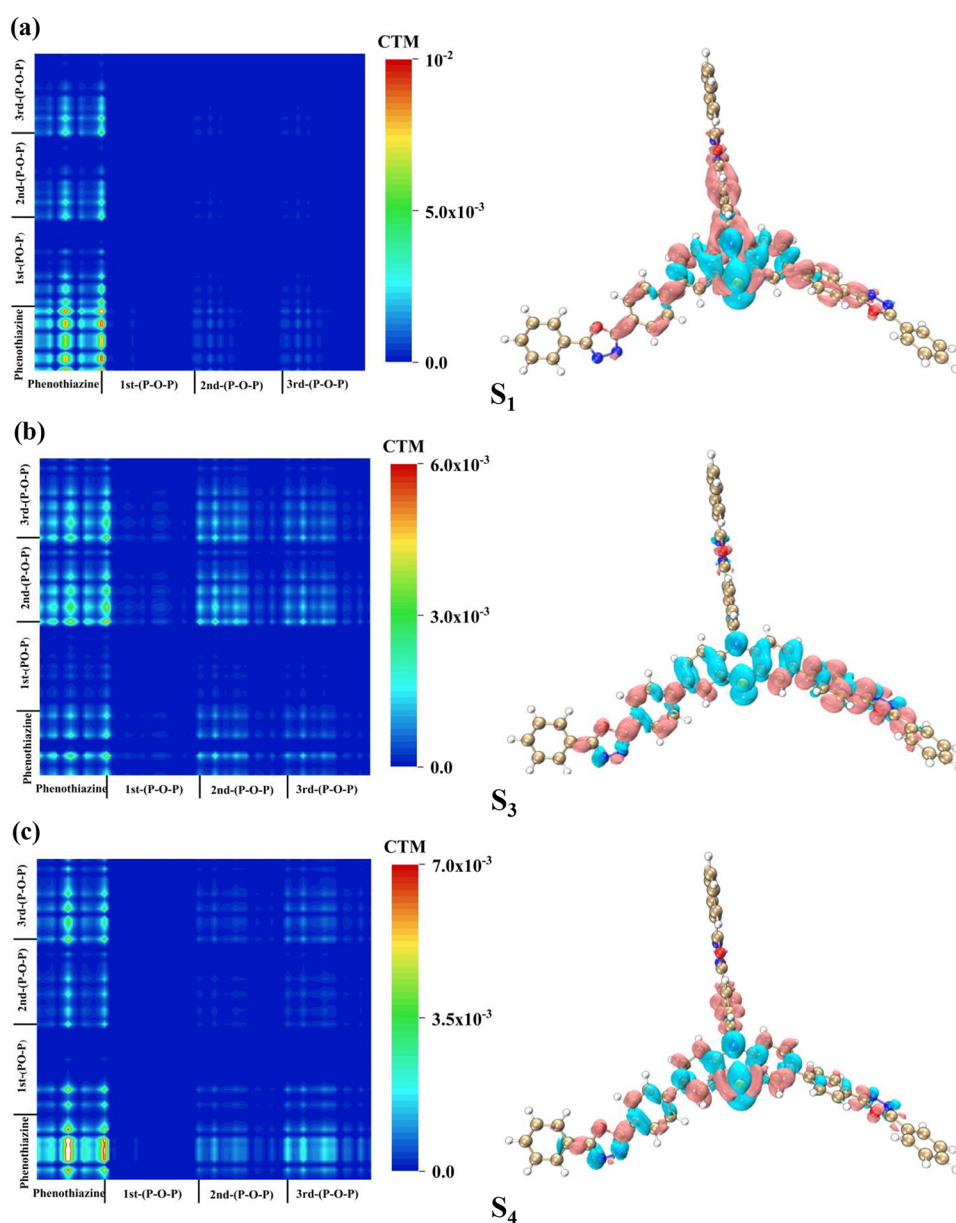
Figure 4. CTM and CDD for the S_1 (a), S_3 (b), and S_4 (c) excited states of TPPO.

fully understand the impact of the increase in the number of branches on charge transfer and to understand the relationship between the structure and properties of charge transfer, one-photon excitation is first analyzed. So, by drawing the CTM and CDD, the charge-transfer characteristics of the two molecules during the OPA process can be analyzed. The CTM diagram can clearly show where and how many electrons are transferred during the electron-excitation process. For M1, the OPA state S_3, which constitutes the lowest energy absorption peak, as well as S_{15} and S_{34} are analyzed, as shown in Figure 3. It can be seen from Figure 3a that only the branched chain has charge transfer. In the CDD of the one-photon excited state of S_3, the pink part in the picture represents electrons (increased electrons) and the blue part represents holes (decreased electrons). The branch is blue-pink, which means that only the branch has increased and decreased electrons, that is, charge transfer. Therefore, combined with the CTM and the CDD, S_3 is locally excited. The CTM and CDD of S_{15} in Figure 3b show the charge transfer within the phenothiazine, but there is also charge transfer from

phenothiazine to the benzene ring of the branch. This shows that the S_{15} excited state is locally excited and supplemented by charge-transfer excitation. For S_{34}, it is mainly charge-transfer excitation, as shown in Figure 3c.

For the TPPO molecule, the analyzed excited states S_3 and S_4 constitute the lowest energy peak and S_1 constitutes the shoulder of the lowest energy peak. Figure 4 shows their CTM and CDD. As seen from the CDD of the S_1 excited state, this is a local excitation on phenothiazine accompanied by a charge-transfer excitation of phenothiazine to the three branches. This can be confirmed from the CTM. Although this excited state has undergone charge transfer, it is only transferred to a part of the acceptor, so local excitation still plays a major role.

We have also analyzed the S_3 excited state of TPPO. The CTM in Figure 4b shows the charge transfer from phenothiazine to the second and third branches. In addition to this, a super-exchange charge-transfer excitation between the second and third branches independent of phenothiazine emerged. It can be seen from the CDD that the branched chain is mainly electrons

and the phenothiazines are mainly holes. That shows these excitation characteristics are dominated by the charge transfer, accompanied by weak local excitation. Comparing the S_3 excited states of the two molecules, M1 is equivalent to the complete local excitation on the first branch, whereas TPPO is accompanied by a super-exchange charge-transfer excitation between the second and third branches independent of the phenothiazine. So, as the number of branches increases, the charge transfer becomes more intense. Comparing the excited states of S_3 and S_4, it can be seen from Figure 4c of CTM and CDD that, unlike S_3, phenothiazine exhibits strong local excitation and a comparably strong charge transfer to the first branch.

3.3. Two-Photon Absorption. According to the TPA spectra of the two phenothiazine derivatives, "three-state" term dominates, indicating that the two-step leap is the major part. This means that TPA will go through an intermediate virtual state and through two transition processes. If the transition probability (transition dipole moment) of these two processes is larger, the TPA excited state with a larger absorption cross section will be observed; so, we can determine the TPA excited state with a larger absorption cross section using the transition dipole moment. For the same two-photon excited state, there will be multiple choices of intermediate states. Therefore, we calculated the transition dipole moments of different paths in the TPA processes of the two molecules to find the intermediate state with the highest probability of appearing in the TPA transition, as shown in Table 1. Using the CDD and TDM of different intermediate states, we visualize the charge-transfer process and intuitively analyze the two-photon transition process.

Table 1. Elements of the TPA Transition Dipole Moment Matrix of M1

molecule	TPA states	process	integral value
M1	S_{17}	$\langle \varphi_{S_0}|\mu|\varphi_{S_3}\rangle \rightarrow \langle \varphi_{S_3}|\mu|\varphi_{S_{17}}\rangle$	9.849−2.7384
	S_{20}	$\langle \varphi_{S_0}|\mu|\varphi_{S_3}\rangle \rightarrow \langle \varphi_{S_3}|\mu|\varphi_{S_{20}}\rangle$	10.185−5.2888
		$\langle \varphi_{S_0}|\mu|\varphi_{S_{16}}\rangle \rightarrow \langle \varphi_{S_{16}}|\mu|\varphi_{S_{20}}\rangle$	1.181−0.596
TPPO	S_8	$\langle \varphi_{S_0}|\mu|\varphi_{S_1}\rangle \rightarrow \langle \varphi_{S_1}|\mu|\varphi_{S_8}\rangle$	8.981−19.575
		$\langle \varphi_{S_0}|\mu|\varphi_{S_3}\rangle \rightarrow \langle \varphi_{S_3}|\mu|\varphi_{S_8}\rangle$	9.849−2.738
	S_{25}	$\langle \varphi_{S_0}|\mu|\varphi_{S_3}\rangle \rightarrow \langle \varphi_{S_3}|\mu|\varphi_{S_{25}}\rangle$	9.849−2.371
		$\langle \varphi_{S_0}|\mu|\varphi_{S_4}\rangle \rightarrow \langle \varphi_4|\mu|\varphi_{25}\rangle$	14.249−5.682
	S_{28}	$\langle \varphi_{S_0}|\mu|\varphi_{S_2}\rangle \rightarrow \langle \varphi_{S_2}|\mu|\varphi_{S_{28}}\rangle$	2.957−4.735
		$\langle \varphi_{S_0}|\mu|\varphi_{S_7}\rangle \rightarrow \langle \varphi_{S_7}|\mu|\varphi_{28}\rangle$	5.724−1.334

According to the TPA spectrum, we analyzed the S_{17} and S_{20} excited states that constitute the strongest absorption peak in the TPA spectrum of M1. According to the transition dipole moment, the intermediate state of the S_{17} excited state of M1 is S_3. According to the previous analysis, the first step, $S_0 \rightarrow S_3$, of this two-photon transition is the complete local excitation in the branch. It can be seen from the TDM in Figure 5a that the second step, $S_3 \rightarrow S_{17}$, is mainly the local excitation of the branched chain, accompanied by the excitation of the charge transfer between phenothiazine and the branched chain. It can be seen from the CDD that electrons are transferred from phenothiazine to the branched chain.

S_3 is also an intermediate state of the S_{20} excited state. Comparing the two transition processes of $S_3 \rightarrow S_{17}$ and $S_3 \rightarrow S_{20}$, it is found that the transition mode is the same, as shown in

Figure 5a,b. It can thus be inferred that the two-photon excited state with S_3 as an intermediate state has the same excitation mode. As shown in Figure 5c,d, for $S_0 \rightarrow S_{16}$, only electrons and holes exist on phenothiazine. CTM shows that only phenothiazine undergoes charge transfer, so this process is a local excitation. In the second step, both are locally excited and there is a charge transfer between the two; it can be seen from the CDD that the electron transfers from the center to the branch chain. Looking at the whole process at a macrolevel, the local excitation in the first step lays the foundation for the charge transfer in the second step. Therefore, it can be considered that the transition is local excitation-enhanced charge-transfer excitation. Therefore, it can be speculated that the TPA charge-transfer mode with different intermediate paths may be quite different.

The TPA spectrum of the molecule TPPO is much more complicated than that of M1, according to the TPA spectrum of TPPO; the S_8 excited state with strong absorption cross sections and S_{25} and S_{28}, which constitute the strongest absorption peaks are analyzed. For the S_8 excited state, we analyzed the excitation characteristics of S_1 and S_3 as the intermediate states. When S_1 is the intermediate state, in the first step, as we analyzed before, the $S_0 \rightarrow S_1$ excitation is characterized by a clear local excitation accompanied by charge transfer from the central molecule to the benzene ring in the first half of the branch, as can be seen in Figure 4a. In the second step, the transition from S_1 to S_8 is also dominated by local excitation, but unlike the first step, the electrons are transferred from the branch to the central molecule, and there is also charge transfer between the branches, as shown in Figure 6a.

The other intermediate state of the S_8 excited state is S_3. As we have analyzed before, $S_0 \rightarrow S_3$ is the charge-transfer excitation, which occurs between the central molecule and the second and third branches. $S_3 \rightarrow S_8$ is the obvious charge-transfer excitation; electrons are transferred from the second and third branches to the central molecule and the first branch. As we can see from Figure 6b, we can get confirmation from the TDM. The charge transfer of the second, third, and first branches proves that the charge transfer between them, which is a kind of super-exchange charge transfer, does not go through the central molecule. In this three-prong D−A structure system, due to the increased versatility of the charge-transfer path, super-exchange charge transfer occurs between the three branches.

The strongest absorption peak of TPPO is contributed by several excited states. We analyzed the S_{25} and S_{28} excited states with relatively large cross sections. First, we analyzed the S_{25} excited state. The intermediate states we chose are S_3 and S_4, and the transition from S_0 to S_3 and S_4 has been discussed, as shown in Figure 4. The TDM and CDD from the intermediate states S_3 and S_4 to S_{25} are shown in Figure 7. The CDD indicates that the electrons of these two paths are transferred from the branch to the central molecule. According to TDM, it can be seen that both have local charge excitation, but in the first path, there is a charge transfer between the first, second, and third branches, that is, super-exchange charge transfer. Therefore, in the excitation process from S_3 to S_{25}, the holes on the single chain are not obvious on CDD.

For the S_{28} excited state, it has two intermediate states, S_2 and S_7. The first and second steps of S_2 as the intermediate excited state are both charge-transfer excitations, as shown in Figure 8. The first step is the transfer of electrons from the central molecule to the three branch chains. It can be seen from the CTM that electrons are transferred from the second and third
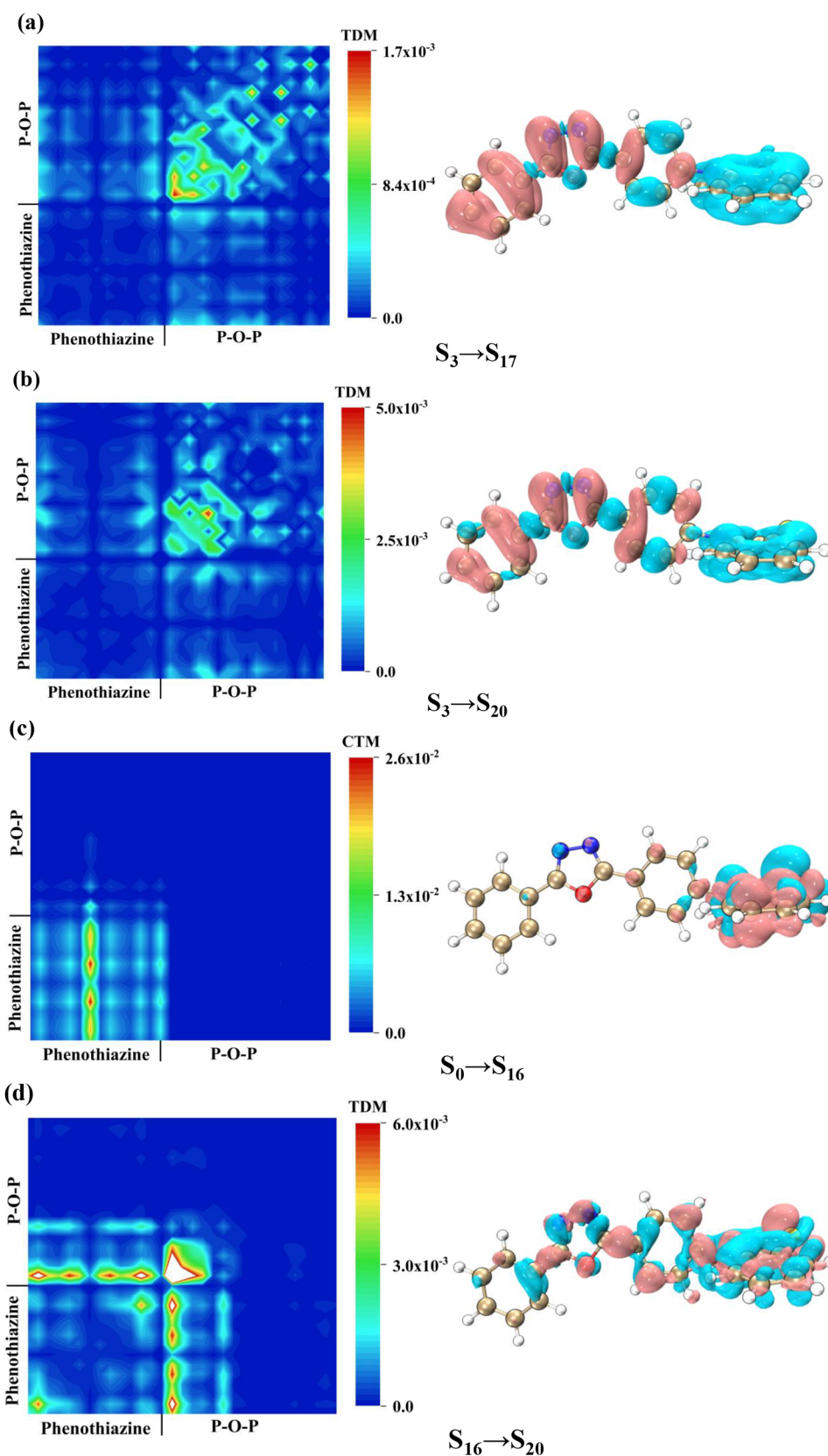
Figure 5. CTM, TDM, and CDD of the two-step process for the S_{17} and S_{20} excited states of M1. The TDM and CDD of (a) $S_3 \rightarrow S_{17}$ and (b) $S_3 \rightarrow S_{20}$. The CTM and CDD of (c) $S_0 \rightarrow S_{16}$ and the TDM and CDD of (d) $S_{16} \rightarrow S_{20}$.

branched chains to the first branched chain, which explains that the isosurface of electrons on the first branched chain in the CDD is relatively large. The second process is the transfer of

electrons from the branched chain to phenothiazine. The charge-movement behavior of these two processes is exactly opposite, that is, the direction of charge transfer is opposite.
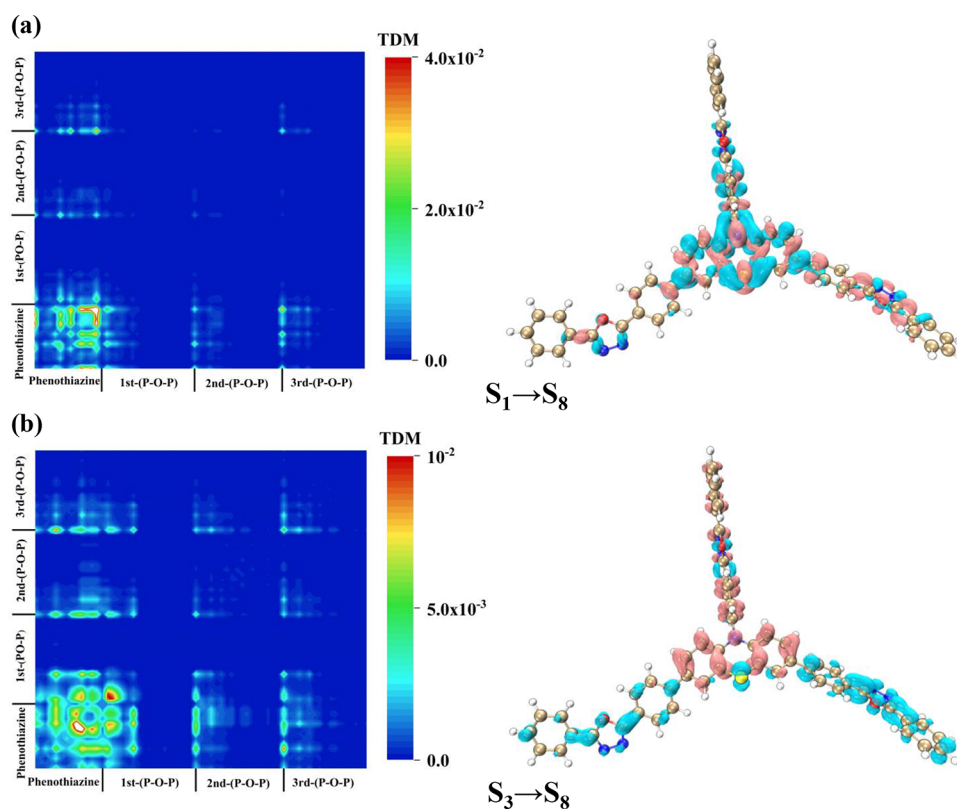
Figure 6. TDM and CDD of the two-step process for the S_8 excited state of TPPO. The TDM and CDD of (a) $S_1 \rightarrow S_8$ and (b) $S_3 \rightarrow S_8$.
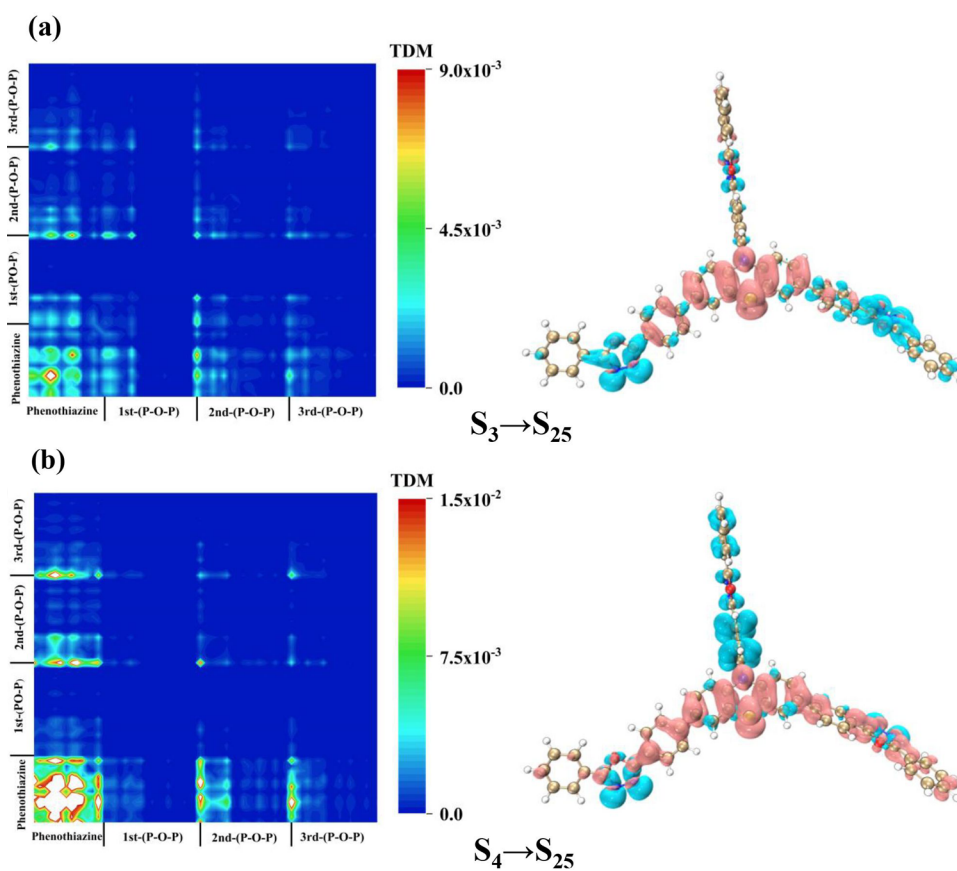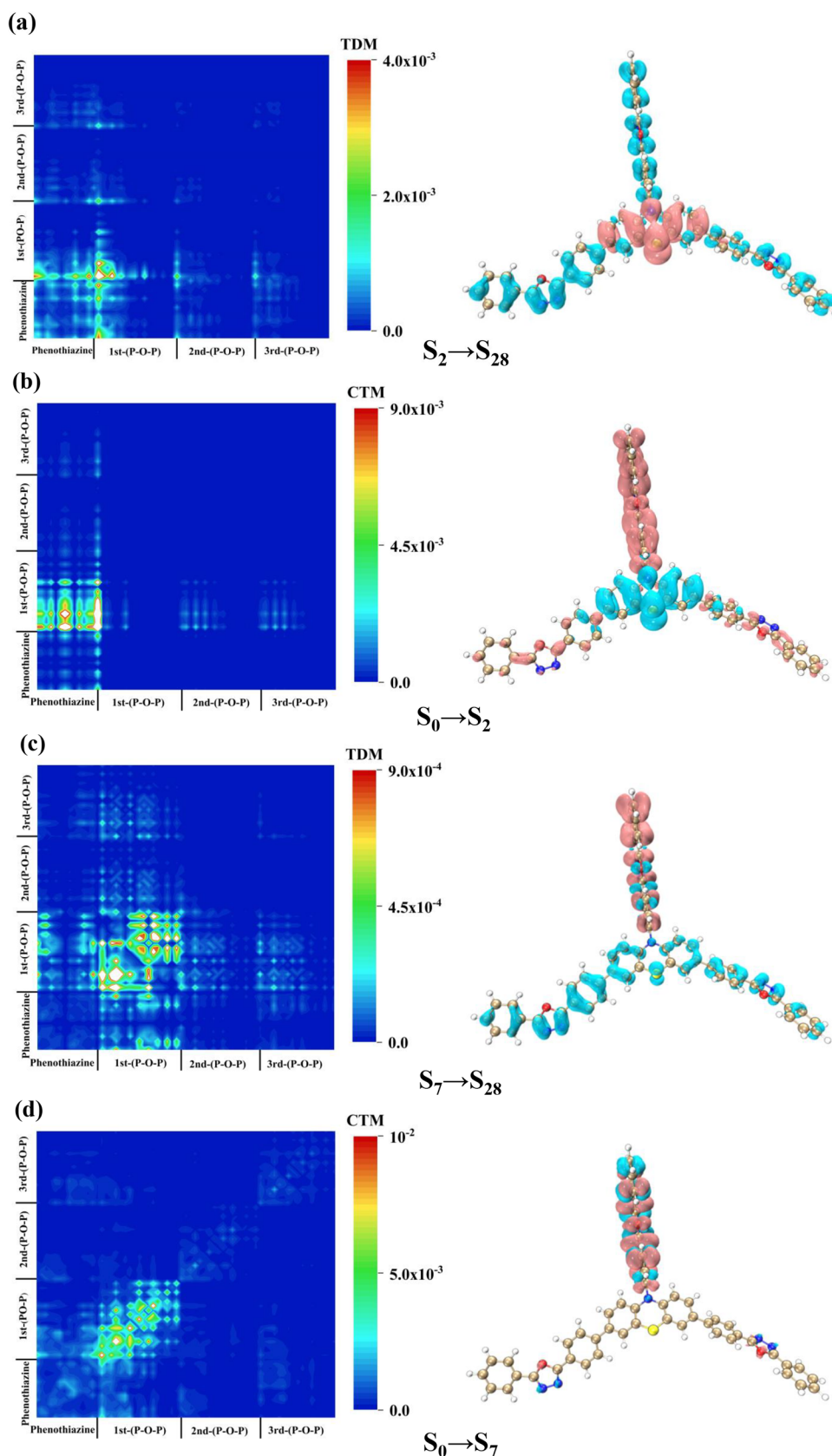

Figure 7. TDM and CDD of the two-step process for the S_{25} excited state of TPPO. The TDM and CDD of (a) $S_3 \rightarrow S_{25}$ and (b) $S_4 \rightarrow S_{25}$.

Figure 8. CTM, TDM, and CDD of the two-step process for the S_{28} excited states of TPPO. The TDM and CDD of (a) $S_2 \to S_{28}$ and (b) $S_0 \to S_2$. The TDM and CDD of (c) $S_7 \to S_{28}$ and the CTM and CDD of (d) $S_0 \to S_7$.

Therefore, S_{28} with S_2 as an intermediate state is a local excitation in the whole process. When the S_7 state is the

intermediate state, it can be seen from the CDD and CTM that the first process, $S_0 \to S_7$, is obvious local excitation at the first

branch. The second process is $S_7 \rightarrow S_{28}$. It can be inferred from CDD shown in Figure 8c that there is not only the charge-transfer excitation from the central molecule to the first branch but also super-exchange charge transfer from the second and third branches to the first branch. However, the local excitation on the first branch cannot be ignored, which can be determined from the TDM. Therefore, for the same excited state, it involves different intermediate states, and its charge-transfer mode is very different. In conclusion, the increase in the number of branches of multibranched compounds during the TPA transition improves the planarity of the system, and the increase in charge-transfer paths allows the molecules to undergo super-exchange charge transfer, resulting in an increase in the TPA cross section.

4. CONCLUSIONS

DFT was used to calculate the OPA and TPA characteristics of organic molecules in the D−A system centered on phenothiazine with strip and trident structures. 2D and 3D visualization methods were used to analyze and discuss two molecules. First, increasing the number of branches significantly promotes the red shift of OPA and TPA peaks. Second, many special charge-transfer modes occur, and local excitation-enhanced charge-transfer excitation occurs in the TPA transition of the strip molecule. In addition, the trident structure shows a super-exchange charge transfer independent of the central molecule, which results in an increase in the absorption cross section. This model has new applications in photocatalysis, organic electronic devices, etc. Our research will further an understanding of the molecular design of multibranched compounds with large cross-sectional TPA.

AUTHOR INFORMATION

Corresponding Authors

Dawei Kang − *College of Physics, Liaoning University, Shenyang 110036, China*; Email: kangdw@lnu.edu.cn

Peng Song − *College of Physics, Liaoning University, Shenyang 110036, China*; ⊙ orcid.org/0000-0003-3093-0068; Phone: +86-24-62202306; Email: songpeng@lnu.edu.cn

Authors

Xinyue Wang − *College of Physics, Liaoning University, Shenyang 110036, China*

Di Wang − *College of Physics, Liaoning University, Shenyang 110036, China*

Jia Li − *College of Physics, Liaoning University, Shenyang 110036, China*

Meixia Zhang − *College of Physics, Liaoning University, Shenyang 110036, China*

Complete contact information is available at:
https://pubs.acs.org/10.1021/acsomega.1c07312

Notes
The authors declare no competing financial interest.

ACKNOWLEDGMENTS

REFERENCES

(1) He, G. S.; Tan, L.-S.; Zheng, Q.; Prasad, P. N. Multiphoton absorbing materials: molecular designs, characterizations, and applications. *Chem. Rev.* **2008**, *108*, 1245−1330.

(2) Göppert-Mayer, M. Über Elementarakte mit zwei quanten-sprungen. *Ann. Phys.* **1931**, *401*, 273−294.

(3) Kaiser, W.; Garret, C. G. B. Two-Photon Excitation in CaF₂: Eu²⁺. *Phys. Rev. Lett.* **1961**, *7*, 229−231.

(4) Li, Y.; Pullerits, T.; Sun, M.; Zhao, M. Theoretical characterization of the PC60BM: PDDTT model for an organic solar cell. *J. Phys. Chem. C* **2011**, *115*, 21865−21873.

(5) Li, Y.; Xu, B.; Song, P.; Ma, F.; Sun, M. D-A-π-A System: Light Harvesting, Charge Transfer and Molecular Designing. *J. Phys. Chem. C* **2017**, *121*, 12546−12561.

(6) Li, Y.; Qi, D.; Song, P.; Ma, F. Fullerene-Based Photoactive Layers for Heterojunction Solar Cells: Structure, Absorption Spectra and Charge Transfer Process. *Materials* **2015**, *8*, 42−56.

(7) Song, P.; Li, Y.; Ma, F.; Pullerits, T.; Sun, M. Photoinduced Electron Transfer in Organic Solar Cells. *Chem. Rec.* **2016**, *16*, 734−753.

(8) Li, R.; Zhang, Y.; Xu, X.; Zhou, Y.; Chen, M.; Sun, M. Optical characterizations of two-dimensional materials using nonlinear optical microscopies of CARS, TPEF, and SHG. *Nanophotonics* **2018**, *7*, 873−881.

(9) Mi, X.; Wang, Y.; Li, R.; Sun, M.; Zhang, Z.; Zheng, H. Multiple surface plasmon resonances enhanced non-linear optical microscopy. *Nanophotonics* **2019**, *8*, 487−493.

(10) Zipfel, W. R.; Williams, R. M.; Webb, W. W. Nonlinear magic: multiphoton microscopy in the biosciences. *Nat. Biotechnol.* **2003**, *21*, 1369−1377.

(11) Helmchen, F.; Denk, W. Deep tissue two-photon microscopy. *Nat. Methods* **2005**, *2*, 932−940.

(12) Xu, L.; Zhang, J.; Yin, L.; Long, X.; Zhang, W.; Zhang, Q. Recent progress in efficient organic two-photon dyes for fluorescence imaging and photodynamic therapy. *J. Mater. Chem. C* **2020**, *8*, 6342−6349.

(13) Ogawa, K. Two-Photon Absorbing Molecules as Potential Materials for 3D Optical Memory. *Appl. Sci.* **2014**, *4*, 1−18.

(14) Li, L.; Wang, P.; Hu, Y.; Lin, G.; Wu, Y.; Huang, W.; Zhao, Q. Novel carbazole derivatives with quinoline ring: synthesis, electronic transition, and two-photon absorption three-dimensional optical data storage. *Spectrochim. Acta, Part A* **2015**, *139*, 243−252.

(15) Cumpston, B. H.; Ananthavel, S. P.; Barlow, S.; Dyer, D. L.; Ehrlich, J. E.; Erskine, L. L.; Heikal, A. A.; Kuebler, S. M.; Lee, I. Y. S.; McCord-Maughon, D.; Qin, J.; Röckel, H.; Rumi, M.; Wu, X.; Marder, S. R.; Perry, J. W. Two-photon polymerization initiators for three-dimensional optical data storage and microfabrication. *Nature* **1999**, *398*, 51−54.

(16) Ogawa, K.; Kobuke, Y. Recent advances in two-photon photodynamic therapy. *Anticancer Agents Med. Chem.* **2008**, *8*, 269−279.

(17) Kim, S.; Ohulchanskyy, T. Y.; Pudavar, H. E.; Pandey, R. K.; Prasad, P. N. Organically modified silica nanoparticles co-encapsulating photosensitizing drug and aggregation-enhanced two-photon absorbing fluorescent dye aggregates for two-photon photodynamic therapy. *J. Am. Chem. Soc.* **2007**, *129*, 2669−2675.

(18) Sun, Z.; Zhang, L.-P.; Wu, F.; Zhao, Y. Photosensitizers for two-photon excited photodynamic therapy. *Adv. Funct. Mater.* **2017**, *27*, No. 1704079.

(19) Shen, Y.; Shuhendler, A. J.; Ye, D.; Jing, J.; Chen, H. Two-photon excitation nanoparticles for photodynamic therapy. *Chem. Soc. Rev.* **2016**, *45*, 6725−6741.

(20) McKenzie, L. K.; Bryant, H. E.; Weinstein, J. A. Transition metal complexes as photosensitisers in one-and two-photon photodynamic therapy. *Coord. Chem. Rev.* **2019**, *379*, 2−29.

(21) Albota, M.; Beljonne, D.; Brédas, J.-L.; Ehrlich Jeffrey, E.; Fu, J.; Heikal Ahmed, A.; Hess Samuel, E.; Kogej, T.; Levin Michael, D.; Marder Seth, R.; McCord-Maughon, D.; Perry Joseph, W.; Röckel, H.; Rumi, M.; Subramaniam, G.; Webb Watt, W.; Wu, X.; Xu, C. Design of organic molecules with large two-photon absorption cross sections. *Science* **1998**, *281*, 1653−1656.

(22) Liang, X.; Zhang, Q. Recent progress on intramolecular charge-transfer compounds as photoelectric active materials. *Sci. China Mater.* **2017**, *60*, 1093−1101.

(23) Pawlicki, M.; Collins, H. A.; Denning, R. G.; Anderson, H. L. Two-photon absorption and the design of two-photon dyes. *Angew. Chem., Int. Ed.* **2009**, *48*, 3244−3266.

(24) Ricci, F.; Elisei, F.; Foggi, P.; Marrocchi, A.; Spalletti, A.; Carlotti, B. Photobehavior and nonlinear optical properties of push-pull, symmetrical, and highly fluorescent benzothiadiazole derivatives. *J. Phys. Chem. C* **2016**, *120*, 23726−23739.

(25) Dereka, B.; Koch, M.; Vauthey, E. Looking at photoinduced charge transfer processes in the IR: answers to several long-standing questions. *Acc. Chem. Res.* **2017**, *50*, 426−434.

(26) Zhang, Y.; Guo, J.; Li, X.; Zhao, M.; Wei, Q.; Song, Peng. One- and two-photon absorption properties of quadrupolar A−π−D−π−A dyes with donors of varying strengths. *Spectrochim. Acta, Part A* **2020**, *230*, No. 118015.

(27) Mu, X.; Wang, X.; Quan, J.; Sun, M. Photoinduced Charge Transfer in Donor-Bridge-Acceptor in One- and Two-Photon Absorption: Sequential and Super-Exchange Mechanisms. *J. Phys. Chem. C* **2020**, *124*, 4968−4981.

(28) Tian, C.; Zhang, Y.; Mu, X.; Quan, J.; Sun, M. Optical Physics on Chiral Brominated Azapirones: Bromophilone A and B. *Spectrochim. Acta, Part A* **2020**, *242*, No. 118780.

(29) Xu, L.; Lin, W.; Huang, B.; Zhang, J.; Long, X.; Zhang, W.; Zhang, Q. The design strategies and applications for organic multi-branched two-photon absorption chromophores with novel cores and branches: a recent review. *J. Mater. Chem. C* **2021**, *9*, 1520−1536.

(30) Qiao, W.; Mu, X.; Zhou, Y.; Wang, J. Physical mechanism of the photoinduced charge transfer in multibranched compounds during one- and two-photon absorption. *Spectrochim. Acta, Part A* **2020**, *231*, No. 118144.

(31) Iqbal, Z.; Wu, W.-Q.; Huang, Z.-S.; Wang, L.; Kuang, D.-B.; Meier, H.; Cao, D. Trilateral π-conjugation extensions of phenothia-zine-based dyes enhance the photovoltaic performance of the dye-sensitized solar cells. *Dyes Pigm.* **2016**, *124*, 63−71.

(32) Lin, R. Y.-Y.; Wu, F.-L.; Li, C.-T.; Chen, P.-Y.; Ho, K.-C.; Lin, J. T. High-Performance Aqueous/Organic Dye-Sensitized Solar Cells Based on Sensitizers Containing Triethylene Oxide Methyl Ether. *ChemSusChem* **2015**, *8*, 2503−2513.

(33) Li, Y.; Li, X.; Xu, Y. A rational design of excellent light-absorbing dyes with different N-substituents at the phenothiazine for high efficiency solar cells. *Spectrochim. Acta, Part A* **2020**, *234*, No. 118241.

(34) Tan, H.; He, J.; Pei, H.; Li, H.; Zhang, S.; Zhang, S. Phenothiazine and Phenoxazine Sensitizer Donor Units:a Comparative Analysis with an Application to Dye-sensitized Solar Cells. *Mater. Rev.* **2018**, *32*, 2538−2541.

(35) Zhao, Y.; Xue, Y.; Sun, J.; Xuan, H.; Xu, Y.; Cui, Y.; Dong, J. A new red fluorescent probe based on the rosamine-phenothiazine for highly selective and rapid detection of hypochlorite and its bioimaging in live cells. *New J. Chem.* **2020**, *44*, 12674−12679.

(36) Vedamalai, M.; Kedaria, D.; Vasita, R.; Gupta, I. Oxidation of phenothiazine based fluorescent probe for hypochlorite and its application to live cell imaging. *Sens. Actuators, B* **2018**, *263*, 137−142.

(37) Ekbote, A.; Mobin, S. M.; Misra, R. Stimuli responsive phenothiazine-based Donor-Acceptor isomers: AIE, Mechanochrom-ism and Polymorphism. *J. Mater. Chem. C* **2020**, *8*, 3589−3602.

(38) Wu, Y.; Shi, J.; Xue, S.; Yang, W. Design, synthesis and mechanochromic luminescence behavior of trigonometric D-A

structures with phenothiazine as center. *China Sciencepaper*. **2017**, http://www.paper.edu.cn/releasepaper/content/201705-484.

(39) Mu, X.; Wang, J.; Sun, M. Visualizations of photoinduced charge transfer and electron-hole coherence in two-photon absorptions. *J. Phys. Chem. C* **2019**, *123*, 14132−14143.

(40) Frisch, M. J.; Schlegel, H. B.; Scuseria, G. E.; Robb, M. A.; Scalmani, G.; Barone, V.; Mennucci, B.; Petersson, G. A.; Caricato, M.; Li, X.; Hratchian, H. P.; Izmaylov, A. F.; Zheng, G.; Sonnenberg, J. L.; Hada, M.; Ehara, M.; Fukuda, R.; Hasegawa, J.; Ishida, M.; Nakajima, T.; Honda, Y.; Nakai, H.; Vreven, T.; Montgomery, J. A., Jr.; Peralta, J. E.; Ogliaro, F.; Bearpark, M.; Heyd, J. J.; Brothers, E.; Kudin, K. N.; Staroverov, V. N.; Kobayashi, R.; Normand, J.; Raghavachari, K.; Rendell, A.; Burant, J. C.; Iyengar, S. S.; Tomasi, J.; Cossi, M.; Rega, N.; Millam, J. M.; Klene, M.; Knox, J. E.; Cross, J. B.; Bakken, V.; Adamo, C.; Jaramillo, J.; Gomperts, R.; Stratmann, R. E.; Yazyev, O.; Austin, A. J.; Cammi, R.; Pomelli, C.; Ochterski, J. W.; Martin, R. L.; Morokuma, K.; Zakrzewski, V. G.; Voth, G. A.; Salvador, P.; Dannenberg, J. J.; Dapprich, S.; Daniels, A. D.; Farkas, O.; Foresman, J. B.; Ortiz, J. V.; Cioslowski, J.; Fox, D. J.; Trucks, G. W.; Cheeseman, J. R.; Nakatsuji, H.; Bloino, J.; Zheng, G.; Toyota, K.; Kitao, O. *Gaussian 09*, Revision D.01; Gaussian Inc.: Wallingford CT, 2013.

(41) Kohn, W.; Sham, L. J. Self-consistent equations including exchange and correlation effects. *Phys. Rev.* **1965**, *140*, A1133−A1138.

(42) Becke, A. D. Density-functional thermochemistry. III. The role of exact exchange. *J. Chem. Phys.* **1993**, *98*, 5648−5652.

(43) Becke, A. D. Density-functional exchange-energy approximation with correct asymptotic behavior. *Phys. Rev. A* **1988**, *38*, 3098−3100.

(44) Gross, E. K. U.; Kohn, W. Local Density-Functional Theory of Frequency-Dependent Linear Response. *Phys. Rev. Lett.* **1985**, *55*, 2850−2852.

(45) Yanai, T.; Tew, D. P.; Handy, N. C. A new hybrid exchange-correlation functional using the Coulomb-attenuating method (CAM-B3LYP). *Chem. Phys. Lett.* **2004**, *393*, 51−57.

(46) Eichkorn, K.; Weigend, F.; Treutler, O.; Ahlrichs, R. Auxiliary basis sets for main row atoms and transition metals and their use to approximate Coulomb potentials. *Theor. Chem. Acc.* **1997**, *97*, 119−124.

(47) Lu, T.; Chen, F. Multiwfn: a multifunctional wavefunction analyzer. *J. Comput. Chem.* **2012**, *33*, 580−592.

(48) Humphrey, W.; Dalke, A.; Schulten, K. VMD: visual molecular dynamics. *J. Mol. Graphics* **1996**, *14*, 33−38.

(49) Sun, M.; Chen, J.; Xu, H. Visualizations of transition dipoles, charge transfer, and electron-hole coherence on electronic state transitions between excited states for two-photon absorption. *J. Chem. Phys.* **2008**, *128*, No. 064106.

(50) Zong, H.; Wang, X.; Quan, J.; Tian, C.; Sun, M. Photoinduced charge transfer by one and two-photon absorptions: physical mechanisms and applications. *Phys. Chem. Chem. Phys.* **2018**, *20*, 19720−19743.

(51) Sun, M.; Ding, Y.; Zhao, L.; Ma, F. Photoexcitation mechanisms of centrosymmetric and asymmetric fluorene derivatives in two-photon absorption. *Chem. Phys.* **2009**, *359*, 166−172.

(52) Wang, C.; Zhao, K.; Su, Y.; Ren, K.; Zhao, X.; Luo, Y. Solvent effects on the electronic structure of a newly synthesized two-photon polymerization initiator. *J. Chem. Phys.* **2003**, *119*, 1208−1213.

(53) Wang, C.; Macak, P.; Luo, Y.; Ågren, H. Effects of π centers and symmetry on two-photon absorption cross sections of organic chromophores. *J. Chem. Phys.* **2001**, *114*, 9813−9820.